

Electronic Supplementary Information

Flexible Lead-Free Piezoelectric Nanogenerator Based on Vertically Aligned BaTiO₃ Nanotube Arrays on Ti-mesh Substrate

Ermias Libnedengel Tsege,^{ad} Gyu Han Kim,^a Venkateswarlu Annapureddy,^b Beomkeun Kim,^c Hyung-Kook Kim^{*a} and Yoon-Hwae Hwang^{*a}

^a Department of Nano Energy Engineering and BK21 Plus Nanoconvergence Technology Division, Pusan National University, Miryang 627-706, South Korea

^b Functional Ceramics Group, Korea Institute of Materials Science (KIMS), Changwon, Gyeongnam 51508, Republic of Korea

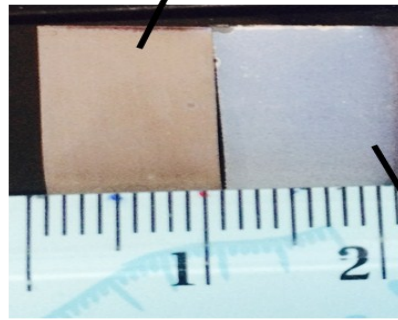
^c High Safety Vehicle Core Technology Research Center, Department of Electronic, Telecommunications, Mechanical & Automotive Engineering, Inje University, 197 Inje-ro, Gimhae, Gyeongnam, 621-749, Korea

^d Department of Physics, Adama Science and Technology University, Adama, Ethiopia.

Corresponding authors: hkkim@pusan.ac.kr (H.-K. Kim), yhwang@pusan.ac.kr (Y.-H. Hwang)

Supporting Information

As grown TiO_2 nanotube film on Ti-foil



As grown BTO nanotube film on Ti-foil

Fig. S1: Photographic image of TiO_2 and BTO nanotube films grown on titanium foil.

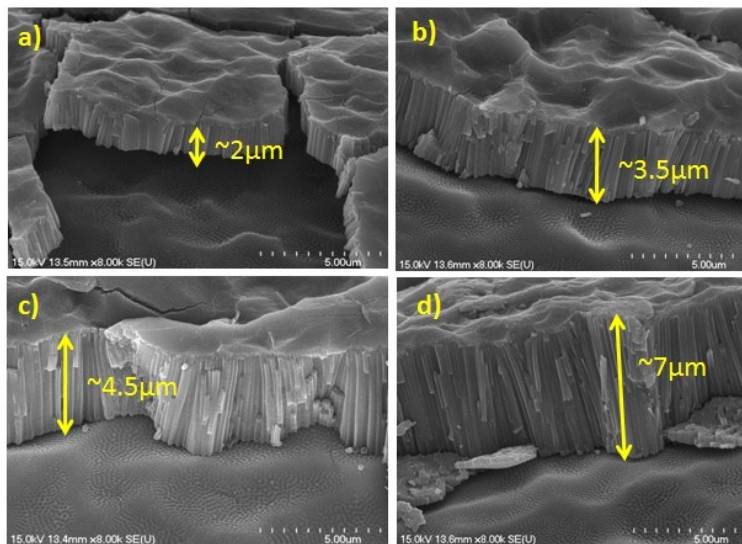


Fig. S2 (a) Cross-sectional SEM image of TiO_2 nanotube arrays grown on Ti-mesh substrate for 2 (a), 4 (b), 6 (c), and 8 hr (d) anodization time

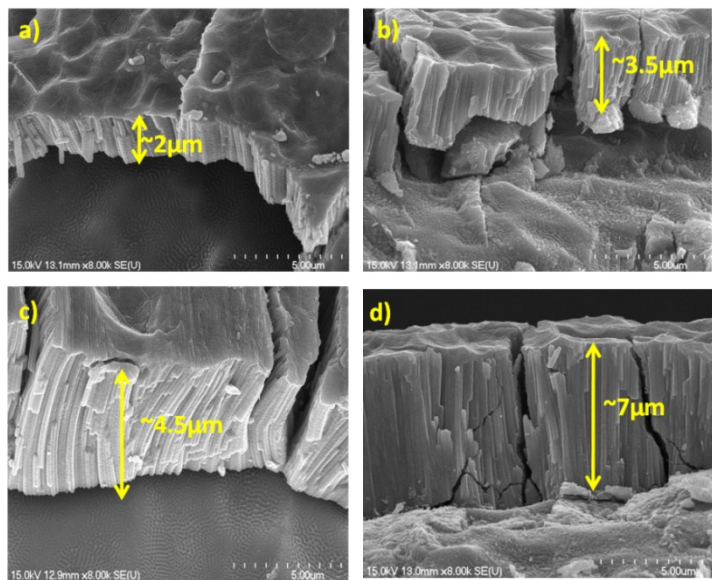


Fig. S3 (a) Cross-sectional SEM image of BTO nanotube arrays on Ti-mesh substrate for 2 (a) 4 (b) 6 (c), and 8 hr (d) anodization time. All the samples are hydrothermally treated for 24 hr in 0.02 M Ba(OH)₂·H₂O solution.

S1. The strain inside the Ti-mesh/BTO-PDMS composite

We analyzed the bending strain in side PDMS encapsulated Ti-mesh/BTO composite (Ti-mesh/BTO-PDMS) due to arbitrary tensile force [1, 2]. We consider cross-sectional part of the PENG device as shown in the schematic diagram (Fig. S4). The strain in the Ti-mesh/BTO-PDMS is defined as:

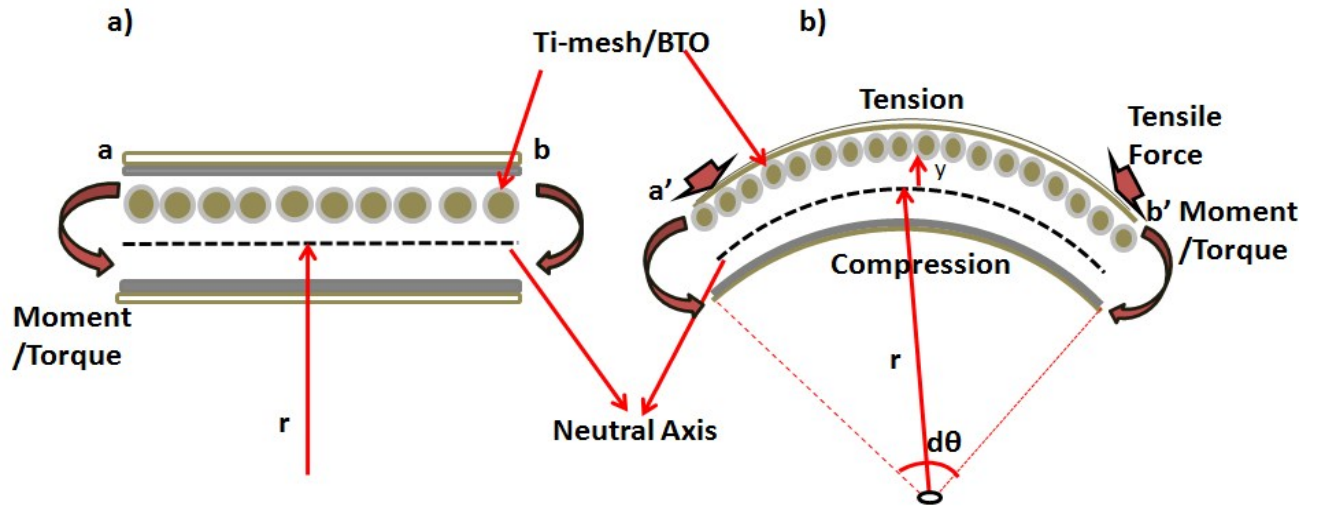


Fig. S4 Schematic of the cross-sectional structure for the Ti-mesh/BTO-based piezoelectric nanogenerator (PENG) in original (a) and bending (b) condition.

$$\varepsilon = \frac{\Delta L}{L} \dots\dots\dots (1)$$

Using the total length of the PENG before bending (ab) and after bending ($a'b'$), we can write equation 1 as:

$$\varepsilon = \frac{a'b' - ab}{ab} \dots\dots\dots (2)$$

The length a'b' can be shorter if it is below the neutral line and longer for above. The radius of curvature r can be written in terms of dθ as:

$$ab = r d\theta \quad \dots\dots\dots (3)$$

$$a'b' = (r + y) d\theta \quad \dots\dots\dots (4)$$

Putting equation 3 and 4 into 2 gives:

$$\boxed{\varepsilon = \frac{y}{r}} \quad \dots\dots\dots (5)$$

Equation 5 indicates the strain at any location inside the Ti-mesh/BTO-PDMS composite film. The equation implies that the strain inside the composite is directly proportional to the distance from the neutral axis (y) and inversely proportional to the radius of curvature (r).

S2. The stress inside the Ti-mesh/BTO-PDMS composite

To understand the relation between the stresses inside Ti-mesh/BTO-PDMS composite it is necessary to write the strain in terms of the stress and moment about the neutral axis. Using Hook's law, $\sigma = E\varepsilon$ we can rewrite equation 5 as:

$$\sigma = \frac{E y}{r} \quad \dots\dots\dots (6)$$

Where, E is Young's modulus and represent ts the stiffness of the material. At equilibrium the total moment about neutral line is given by:

$$\sum M_{neutral\ line} = 0 \quad \dots\dots\dots (7)$$

$$\int y (dF) = M \dots\dots\dots (8)$$

S5

Where, F is the force at small area dA. Using the relation $F/dA = \sigma$ we can write equation 8 as:

$$\int y \sigma dA = M \dots\dots\dots (9)$$

This equation can be rewrite using equation 6 to give:

$$\frac{E}{r} \int y^2 \sigma dA = M \dots\dots\dots (10)$$

Using area moment of inertia $I = \int y^2 dA$ we can write equation 10 as:

$$\sigma_{bending} = \frac{M Y}{I}$$

$$\dots\dots\dots (11)$$

Equation 11, implies that the stress inside the Ti-mesh/BTO-PDMS composite is depend on the distance from the neutral line, y. Both equation 5 and 11, indicates that the strain and stress inside the Ti-mesh/BTO-PDMS composite directly related to the position of the piezoelectrically active layer from the neutral line. Therefore, unsymmetrical positioning of the piezoelectrically active layer induces high stress on the piezoelectrically active layer during bending and gives rise to higher piezoelectric output.

S6

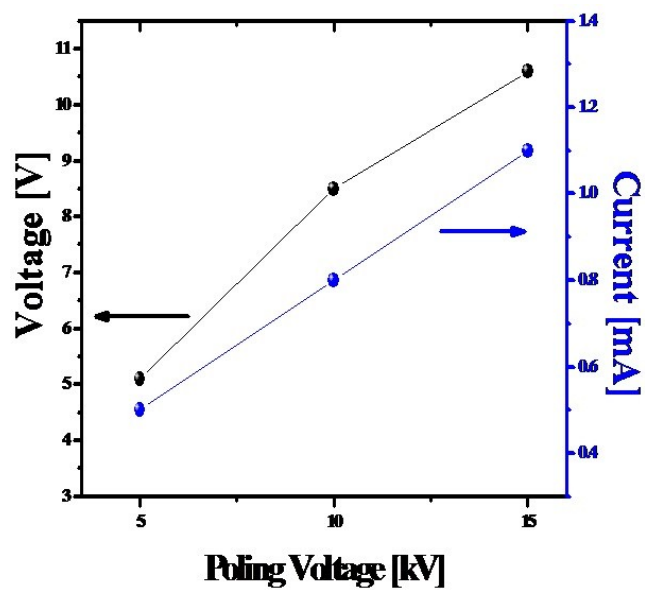


Fig. S5 Output voltage and current generated from the Ti-mesh/BTO- based nanogenerator as a function of poling voltage.

S7

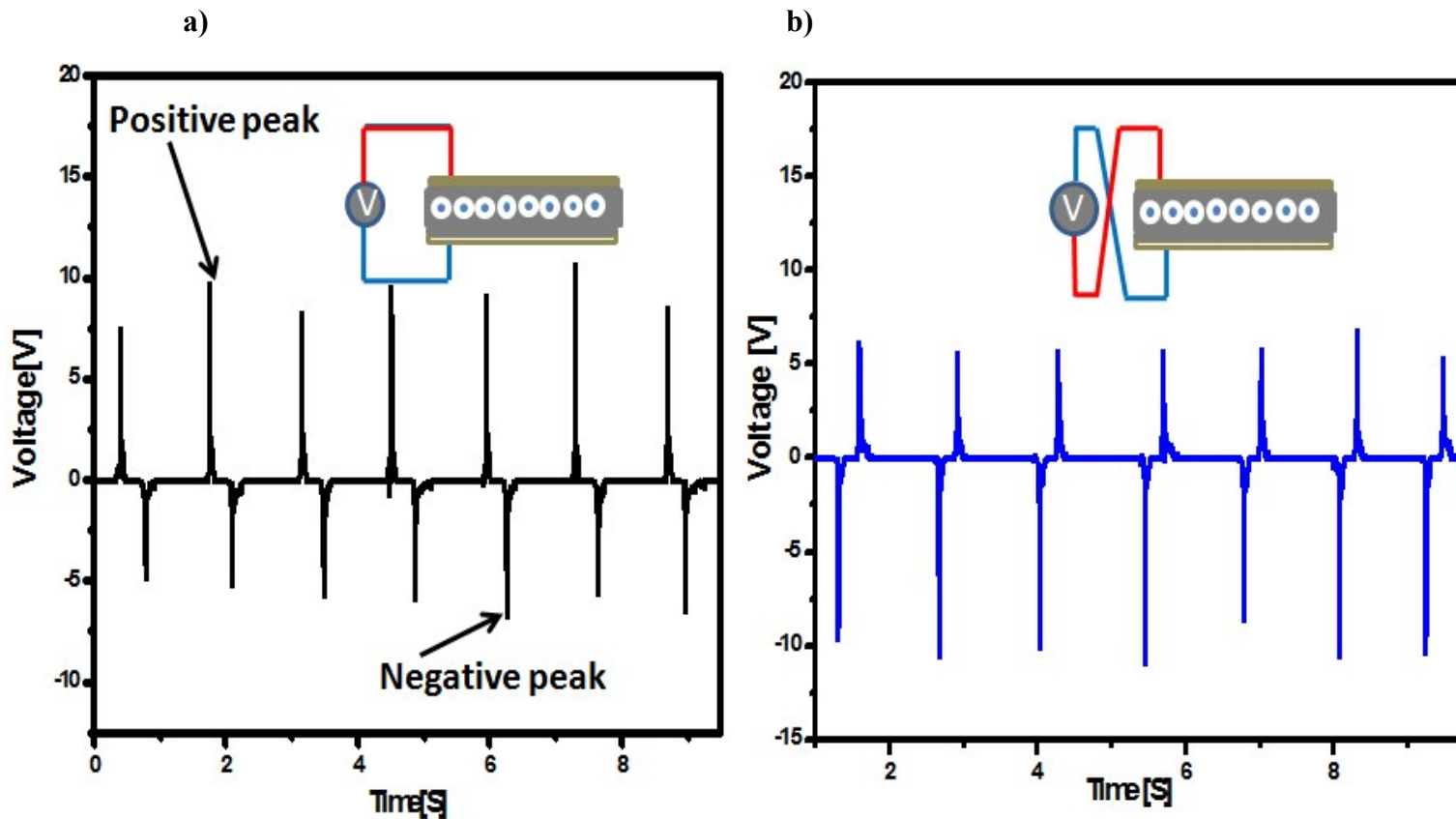


Fig. S6 Measured output voltage of the PENG due to bending and releasing condition, at a frequency of 0.7 Hz during forward (a) and reverse (b) connection to the measuring device.

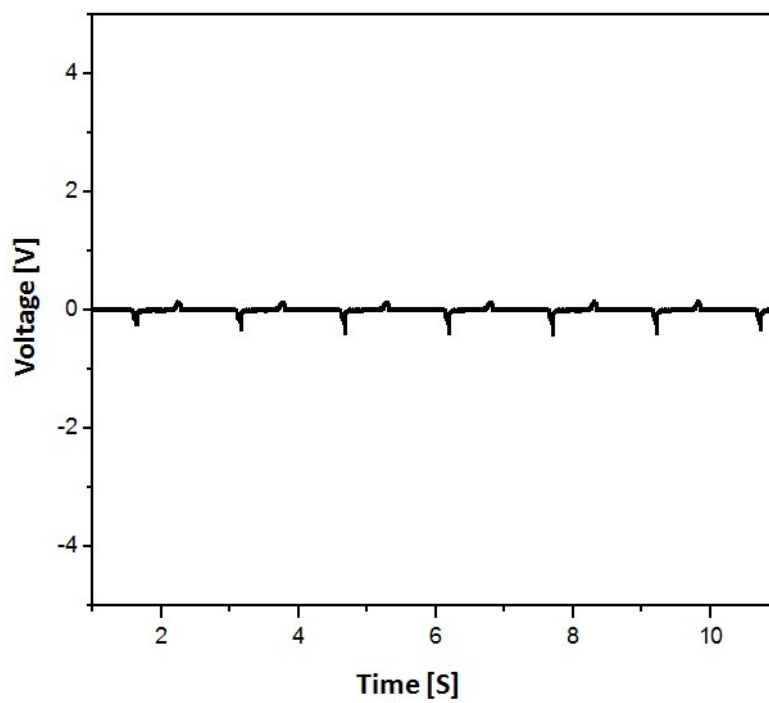


Fig. S7 Output voltage of the PENG device without the Ti-mesh/BTO active layer under bending and releasing motion at a frequency of 0.7 Hz.

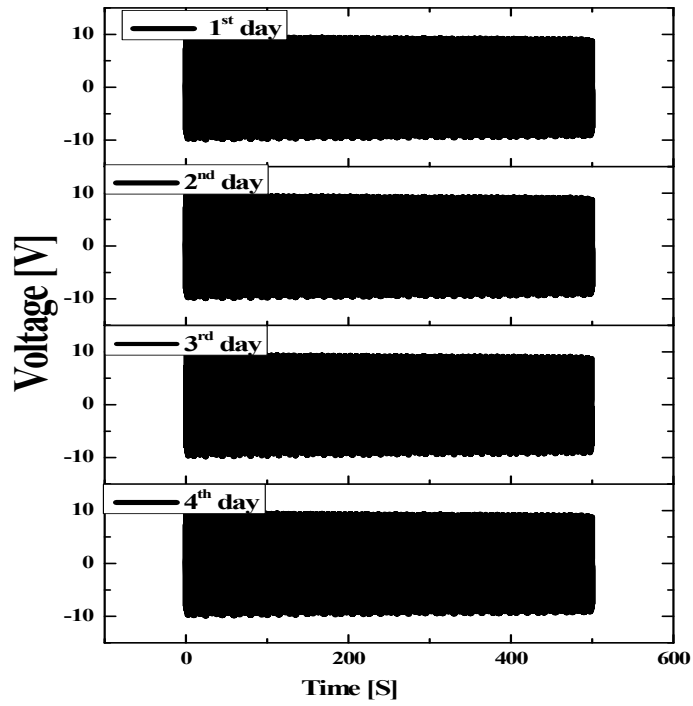


Fig. S8 Stable output voltage generation test for four different days for a total of 2800 cycles.

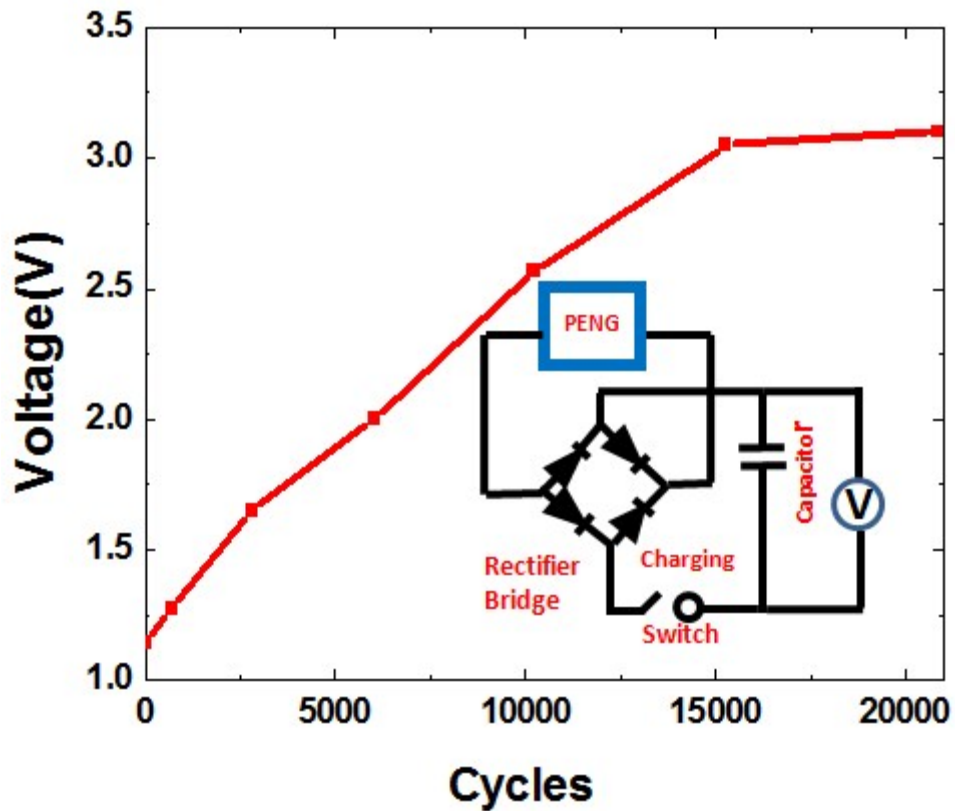


Fig. S9 The charging curve of 10 μ F capacitor charged by Ti-mesh/BTO-based PENG device. The inset shows the bridge rectifier circuit diagram used for charging the capacitor.

Materials	Composite Nanostructures	Applied Stress	Maximum Output Voltage (V)	Reference
Alkaline niobate (KNLN)	KNLN particles with Cu nanorods	bending	12	3
BTO	nanowires	bending	7	4
BTO	Virus-templated nanostructures	bending	6	5
BTO	nanoparticle	bending	5	6
BTO	nanoparticle	bending	3	7
BTO	self-assembled BTO film	bending	6.5	8
BTO	Ti-mesh/BTO nanotube arrays	bending	10.6	This work

Table S1. Performance comparison with other reported flexible lead-free composite-based nanogenerators.

References

- [1] E. P. Popov, S. Nagarajan, Z. A. Lu. "Mechanics of Material". Englewood Cliffs, N.J.: Prentice-Hall, ©1976
- [2] <http://creativecommons.org/licenses/by-nc-nd/4.0/>
- [3] C. K. Jeong, K.-I. Park, J. Ryu, G.-T. Hwang, K. J. Lee, *Adv. Funct. Mater.* 2014, **24**, 2620–2629.
- [4] K. -I Park, S. B. Bae, S. H. Yang, H. I. Lee, K. Lee and S. J. Lee, *Nanoscale*, 2014, **6**, 8962–8968.(nanowire)
- [5] C. K. Jeong, I. Kim, K. I. Park, M. H. Oh, H. Paik, G. T. Hwang, K. No, Y. S. Nam, K. J. Lee, *ACS Nano*, 2013, **7**, 11016–11025
- [6] S. H. Shin, Y. H. Kim, M. H. Lee, J. Y. Jung, J. Nah, *ACS Nano*, 2014, **8**, 2766–2773.
- [7] K. I. Park , M. Lee, Y. Liu, S. Moon, G. T. Hwang, G. Zhu, J. E. Kim, S. O. Kim, D. K. Kim, Z. L. Wang, K. J. Lee, *Adv. Mater.*, 2012, **24**, 2999-3004.
- [8] T. Gao, J. Liao, J. Wang, Y. Qiu, Q. Yang, M. Zhang, Y. Zhao, L. Qin, H. Xue, Z. Xiong, L. Chena and Q. –M Wang, *J. Mater. Chem. A*, 2015, **3**, 9965–9971.